Electronic Supplementary Material (ESI) for Journal of Materials Chemistry C.

Supplementary Information

Antiferromagnetic Single-Chain Magnet slow relaxation in the $\{Tb(\alpha\text{-fur})_3\}_n$ polymer with non-Kramers ions

E.Bartolomé*[a] , J. Bartolomé [b] , A. Arauzo[b,c], J. Luzón[d], L. Badía[b], R. Cases[b], F. Luis[b] , S. Melnic[e], D. Prodius[e], S. Shova[f] and C. Turta[e+]

S1. *Ab initio* calculations

In the {Tb(α-fur)$_3$} complex, random disorder between one water molecule and one of the dangling ligands results in two slightly different Tb environments, Tb(A) and Tb(B). This structural difference can be well appreciated in the *ab*-plane projection (Figure S1). We have used *ab initio* calculations to determine the ligand field (LF) split eigenstates and eigenvalues of the two Tb sites. The LF eigenstates are expressed as linear combinations of the $|J,M_J\rangle$ (J=6,M_J=+6, …, -6) angular moment wave functions with respect to the quantization axis, defined by the principal axis of the *g** tensor: $|\xi_i\rangle = \sum_{M=-J}^{J} C^i_{J,M_J}|J,M_J\rangle$. The |J, M_J> decomposition of the four lowest energy levels are summarized in Tables S1 (Tb site A) and Table S2 (Tb site B). In each state, the first number is the real component of the coefficient and the second is the imaginary part. The phase is chosen such that |6,6> vector has only real part.

M_J	**Ground state** $\|\xi_0\rangle$		**1st excited level** $\|\xi_1\rangle$		**2nd level** $\|\xi_2\rangle$		**3rd level** $\|\xi_3\rangle$	
C^i_{J,M_J}	***Real***	***Imaginary***	***Real***	***Imaginary***	***Real***	***Imaginary***	***Real***	***Imaginary***
-6	-0.1602	-0.6229	-0.1605	-0.6229	-0.2274	-0.0659	0.2295	0.0831
-5	-0.2140	0.0499	-0.2163	0.0496	0.2003	-0.5335	-0.2448	0.5394
-4	-0.0080	0.1581	-0.0060	0.1566	0.0282	-0.0424	0.0006	0.0445
-3	0.0830	0.0392	0.0819	0.0430	-0.0481	0.2353	0.0101	-0.1772
-2	0.0430	-0.0265	0.0396	-0.0260	0.0436	0.2100	0.0169	-0.1923
-1	0.0049	-0.0409	-0.0076	-0.0331	-0.0805	0.0668	-0.0715	-0.1131
0	-0.0144	0.0185	-0.0244	-0.0189	0.0089	-0.0625	0.0409	0.0072
1	-0.0384	0.0150	0.0339	-0.0009	-0.0587	-0.0866	0.1057	-0.0820
2	0.0149	-0.0483	-0.0153	0.0448	-0.1004	0.1896	-0.0496	0.1865
3	0.0586	0.0706	-0.0620	-0.0686	0.0193	-0.2394	0.0508	-0.1701
4	-0.1511	0.0471	0.1502	-0.0449	-0.0152	-0.0485	0.0157	-0.0412
5	-0.0049	-0.2197	0.0059	0.2219	0.0438	0.5682	0.0466	0.5905
6	0.6432	0.0000	-0.6432	-0.0000	0.2368	0.0000	0.2441	0.0000

Table S1. |J, M_J> decomposition of the four lowest energy levels for Tb(A)

M_J	**Ground state** $\|\xi_0\rangle$		**1st excited level** $\|\xi_1\rangle$		**2nd level** $\|\xi_2\rangle$		**3rd level** $\|\xi_3\rangle$	
C^i_{J,M_J}	***Real***	***Imaginary***	***Real***	***Imaginary***	***Real***	***Imaginary***	***Real***	***Imaginary***
-6	0.0625	-0.6127	-0.0607	0.6127	0.2422	0.0184	0.2459	-0.0167
-5	0.1868	-0.2302	-0.1901	0.2312	-0.3594	-0.3034	-0.4027	-0.2824
-4	0.1255	0.0132	-0.1268	-0.0100	0.1215	-0.0158	0.1422	-0.0153
-3	0.0146	0.1059	-0.0062	-0.1037	-0.1468	-0.1235	-0.1288	-0.1905
-2	-0.0663	0.0108	0.0529	-0.0212	0.2678	0.2417	0.1966	0.1133
-1	-0.0096	0.0025	0.0072	0.0328	-0.1239	0.0072	-0.2677	-0.0177
0	0.0300	-0.0271	0.0048	0.0053	0.2119	0.0081	-0.0012	-0.0338
1	0.0035	-0.0093	-0.0320	-0.0104	0.1230	0.0166	-0.2659	0.0360
2	-0.0174	0.0648	-0.0263	0.0505	0.2854	-0.2207	-0.1883	0.1265
3	0.1039	0.0253	0.1025	0.0164	0.1557	-0.1120	-0.1154	0.1989
4	-0.0004	-0.1262	0.0025	-0.1272	0.1199	0.0250	-0.1429	-0.0055
5	-0.2480	0.1625	-0.2488	0.1664	0.3813	-0.2752	-0.3823	0.3094
6	0.6159	0.0000	0.6157	0.0000	0.2429	0.0000	-0.2465	0.0000

Table S2. |J, M_J> decomposition of the four lowest energy levels for Tb(B)

Table S3 summarizes the calculated energy levels produced by LF splitting for the two sites.

E(K) Tb(A)	E(K) Tb(B)
0	0
0.201=Δ_A/k_B	0.258=Δ_B/k_B
185.9	168.8
188.4	173.6
232.4	199.9
245.4	214.6
310.3	283.9
338.9	302.0
378.8	321.4
421.0	377.3
434.9	379.9
471.0	465.7
473.9	466.4

Table S3. LF split energy levels (in K units) for Tb(III) in the two possible sites A and B.

The ground state singlet $|\xi_0\rangle$ and the first excited one $|\xi_1\rangle$ are separated by an energy $E_1 \equiv \Delta < 1$K, much smaller than the energy E_2 (160-180 K) of the next state $|\xi_2\rangle$. Thus, at sufficiently low temperatures $k_B T << E_2$ only the two lowest states are populated, so it is admissible to use the effective S*=1/2 description. The single ion LF Hamiltonian can be expressed in this subspace as:

$$\hat{H}_{LF}^{*} = \Delta \begin{pmatrix} 00 \\ 01 \end{pmatrix}, \qquad [S.1]$$

where the asterisk indicates the projection on the two lowest states. In the case of ions with an even number of unpaired electrons, such as Tb(III), it has been shown[1] that when the excited states above the quasi-doublet are at much higher energy, thus avoiding the mixing of states, the ground state has uniaxial anisotropy. This result is actually obtained in our *ab initio* calculations with $g_z^* \neq 0$, $g_x^* = g_y^* = 0$, with *z* nearly perpendicular to the *c* crystallographic direction (Table S4).

	Tb(A)	Tb(B)
g_x^*	0.0	0.0
g_y^*	0.0	0.0
g_z^*	17.8	17.8

Table S4. *Ab initio* calculated gyromagnetic values for Tb sites A and B.

It is convenient to apply a base change transformation, *R*:

$$|\eta\rangle = \frac{1}{\sqrt{2}}(|\xi_0\rangle + |\xi_1\rangle) \text{ and } |\Sigma\rangle = \frac{1}{\sqrt{2}}(|\xi_0\rangle - |\xi_1\rangle). \qquad [S.2]$$

diagonalising the Zeeman splitting under an intense applied magnetic field and maximising the $\hat{J}_\alpha$ eigenvalues: $\hat{J}_z|\eta\rangle \approx +6|\eta\rangle$ and $\hat{J}_z|\Sigma\rangle \approx -6|\Sigma\rangle$. Table S5 shows the module and phase of the wave functions, $|\eta\rangle$ and $|\Sigma\rangle$, for the two Tb sites.

	Tb(A)					Tb(B)			
M_J	**Ground state** $\|\eta\rangle$		**1st excited level** $\|\Sigma\rangle$			**Ground state** $\|\eta\rangle$		**1st excited level** $\|\Sigma\rangle$	
	Module	***Phase***	***Module***	***Phase***		***Module***	***Phase***	***Module***	***Phase***
-6	**0,9096**	-1,8228	0,0002	-0,0800		0,0013	-0,0272	**0,8708**	-1,4706
-5	0,3124	2,9141	0,0017	0,1305		0,0024	2,8554	0,4213	-0,8859
-4	0,2228	1,6153	0,0018	2,5052		0,0024	1,9588	0,1791	0,0918
-3	0,1303	0,4619	0,0028	-1,2904		0,0062	0,2619	0,1489	1,4717
-2	0,0692	-0,5660	0,0025	-0,1501		0,0120	-2,4789	0,0872	2,8793
-1	0,0524	-1,6073	0,0105	-0,5600		0,0251	1,6379	0,0245	-2,0768
0	0,0274	-3,1317	0,0274	1,3089		0,0291	-0,5588	0,0290	-0,9104
1	0,0105	1,8792	0,0524	2,9262		0,0245	-2,5366	0,0251	0,0319
2	0,0025	-1,6684	0,0692	-1,2568		0,0872	1,9335	0,0119	1,0147
3	0,0028	2,6078	0,1303	0,8569		0,1489	0,1993	0,0064	1,4210
4	0,0017	1,9681	0,2228	2,8451		0,1791	-1,5624	0,0022	2,8192
5	0,0017	1,1600	0,3124	-1,5953		0,4213	2,5569	0,0028	-1,3634
6	2,616E-05	3,1416	**0,9096**	0		**0,8708**	0	0,0002	0

Table S4. Ground state and 1st excited level wave functions after the *R* base change, for Tb(A) and Tb(B).

The direction of the Easy Axes of Magnetization (EAM) as calculated by *ab initio* for A and B sites are shown in Figure S1. For both sites the EAM is close to the *a** direction, almost perpendicular to the chain direction (*c*-axis): 87.9º and 80.1º, for Tb(A) and Tb(B), respectively. It is concluded that the interchange of a water molecule by one of the ligands produces only small differences in the energy levels, nature of the states or in the direction of the EAM.

XRD shows that within one chain, all Tb sites are of the same type. Thus the LF Hamiltonian for each Tb, projected onto the restricted subspace $|1/2,\pm 1/2\rangle$ of the complete basis, is:

$$\hat{H}^{*}_{LF(A,B)} = \sum_{i=1}^{N} \Delta_{A,B} \hat{S}^{*}_{i,\perp}, \qquad [S.3]$$

where i runs along the sites, and A and B for the two types of sites.

Tb A:

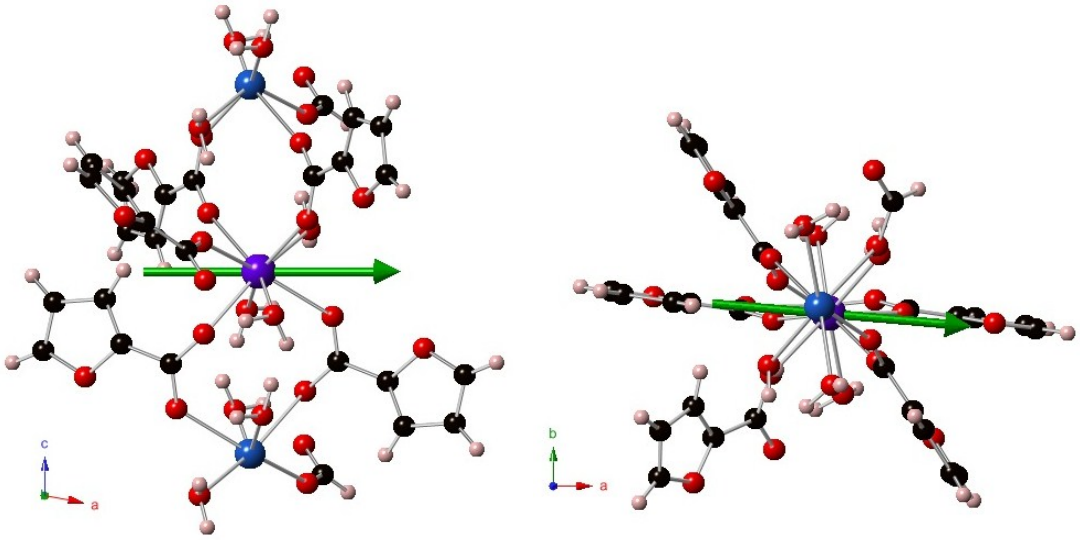

Tb B:

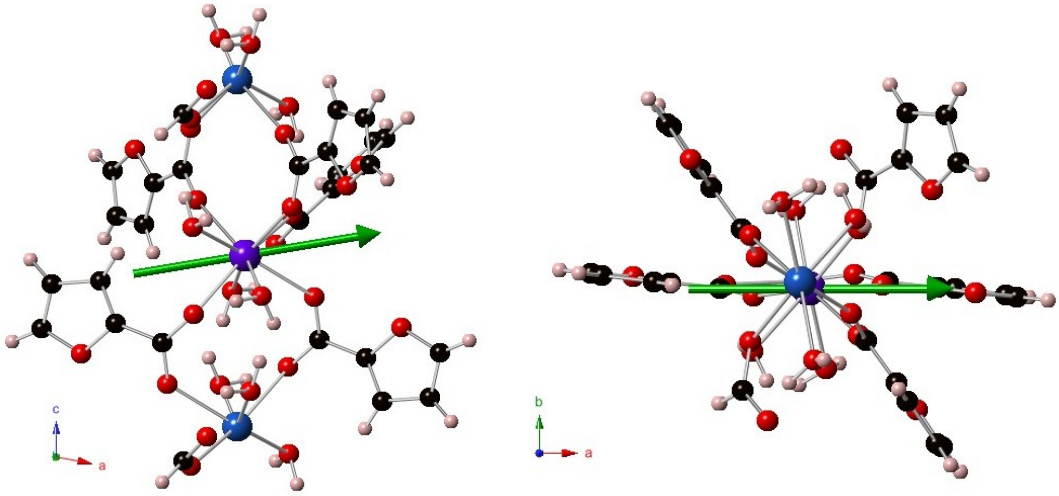

Figure S1. Direction of the calculated EAM for both Tb sites, A and B.

S2. ***Single-ion relaxation of non-Kramers ions by tunnelling***

In the case of Kramers ions, pure quantum tunnelling of the magnetization (QTM) between the degenerate doublet ground state is forbidden, unless an external perturbation, ξ_{dip}, caused by dipolar, hyperfine or external field allow it. For non-Kramers ions, by contrast, the ZFS energy gap between the quasi-doublet plays the role of a bias field, that may fall within the threshold of $\xi_{bias} = \Delta + \xi_{dip} \leq \Delta_t$ for tunnelling to take place. Here ξ_{dip} encompasses perturbations due to dipolar, exchange and hyperfine interactions, while Δ_{t} contains the effects of transversal magnetic fields. Under these conditions the prediction for the tunnelling rate through the lowest two states is:

$$\tau_{\mathrm{t}} \approx \frac{\mathrm{h}}{\Delta_{\mathrm{t}}^2 P\left(\xi_{dip}\right)}. \qquad [S.1]$$

The Tb nuclear moment I=3/2 coupled to the electronic states yields an important effect to the bias field and may enhance the tunnelling probability.

Thermally activated quantum tunnelling (TAQT) has the same temperature dependence as an Orbach process (Eq. 11), provided there exist excited degenerate electronic levels. In our complex, none of these processes were observed.

S3. Dynamic magnetic measurements

Figure S2 shows ac susceptibility measured in the SQUID at different frequencies in the temperature range 1.8 - 15 K, in zero-field. The out-of-phase susceptibility showed a small frequency dependent signal, though peaks could not be observed down to the lowest measured *T*. This led us to make measurements down to lower temperatures in the dilution refrigerator.

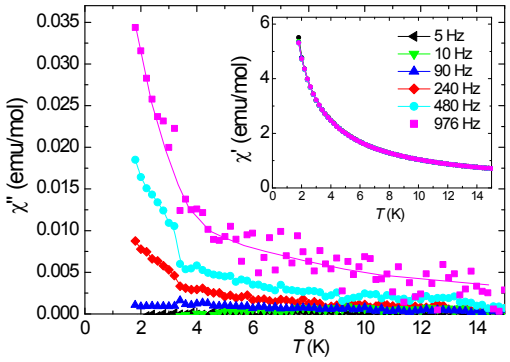

Figure S2. χ', $\chi''(T)$ at different frequencies at H=0 measured by SQUID between 1.8 - 15K.

Figure S3 shows the $\chi'(f)$, $\chi''(f)$ susceptibility curves at different isotherms, measured with the microSQUID installed in the dilution refrigerator. Two slow relaxation processes are distinguished.

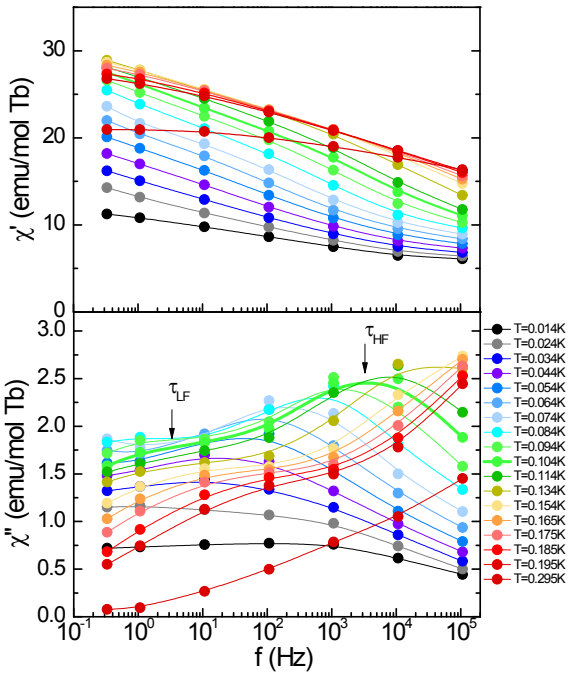

Figure S3. χ', $\chi''(T)$ at different constant temperatures at H=0 measured by a microSQUID in a dilution refrigerator.

References

1 J. S. Griffith, *Phys. Rev.*, 1963, **132**, 316–319.